Biochemical and Biophysical Research Communications 462 (2015) 58–63

Contents lists available at ScienceDirect

Biochemical and Biophysical Research Communications

journal homepage: www.elsevier.com/locate/ybbrc

The relationship between glycan structures and expression levels of an endoplasmic reticulum-resident glycoprotein, UDP-glucose: Glycoprotein glucosyltransferase 1

Shusaku Daikoku [a], Akira Seko [a, *], Sang-Hyun Son [a], Katsuhiko Suzuki [a], Yukishige Ito [a, b], Osamu Kanie [a, c, *]

[a] ERATO, Japan Science and Technology Agency (JST), Ito Glycotrilogy Project, 2-1 Hirosawa, Wako, Saitama 351-0198, Japan
[b] Synthetic Cellular Chemistry Laboratory, RIKEN, 2-1 Hirosawa, Wako, Saitama 351-0198, Japan
[c] Tokai University, Institute of Glycoscience, 4-1-1 Kitakaname, Hiratsuka, Kanagawa 259-1292, Japan

ARTICLE INFO

Article history:
Received 7 April 2015
Available online 29 April 2015

Keywords:
Uridine 5′-diphosphate-glucose: glycoprotein glucosyltransferase 1
Expression level
NanoLC–tandem MS

ABSTRACT

In this article, we report a relationship between glycan structures and expression levels of a recombinant ER-resident glycoprotein, uridine 5′-diphosphate-glucose: glycoprotein glucosyltransferase (UGGT1). The function of glycan structures attached to a glycoprotein is actively studied; however, the glycan structures of recombinant, and not endogenous, glycoproteins have not been examined. In this study, we indicate a relationship between the glycan structure and the level of protein expression. Expression levels were controlled utilizing a series of vectors (pFN21K, pFN22K, pFN23K, and pFN24K HaloTag CMV Flexi Vectors). Qualitative and semi-quantitative confirmation of glycan structures was achieved with tandem mass spectrometry. The results of this study indicate that glycan structures are similar to endogenous glycans at low expression levels.

1. Introduction

Glycosylation is one of the important post-translational modifications (PTM) in a wide variety of proteins [1,2]. This process has received attention recently due to the development of protein-based pharmaceuticals, including erythropoietin and antibodies, that require such modifications [3,4]. Since most secreted and membrane-bound proteins are glycosylated, and because changes in glycan structure have been reported to affect protein function, post-translational quality control in research and development is critical [5]. Despite this importance of glycan structure, there is often virtually no information available on the mechanism underlying the expression of glycoproteins and about the details of glycoforms produced in an experimental procedure.

Glycans are covalently bound to asparagine (*N*-linked glycosylation) or to serine/threonine (*O*-linked glycosylation) [6]. In the endoplasmic reticulum (ER), the glycans transferred from a dorichol-linked precursor onto nascent polypeptides serve as tag-moieties, representing the folding status of polypeptide chains of glycoproteins. The process is called the ER quality control (ERQC) system [7,8]. Some chaperones, such as glucosidases, glucosyltransferases, and protein disulfide isomerases, that play important roles in ERQC are known to be glycoproteins themselves [9,10]. For example, uridine 5′-diphosphate (UDP)-glucose: glycoprotein glucosyltransferase 1 (UGGT1) acts as a folding sensor. The glucosyltransferase is a pivotal enzyme that is responsible for the re-glucosylation of Man9GlcNAc2 glycan-producing GlcManGlcNAc2. This ensures that misfolded proteins are recognized by and reassociated with the glycan-recognising chaperones calnexin and/or calreticulin [11]. However, biological functions of these glycoproteins in ERQC have not been fully elucidated, partly because the number of ER-resident glycoproteins is often very small. We have engaged in the challenge of elucidating the role of UGGT1 in ERQC, and, previously, we reported the glycan structure and its

Abbreviations: Hex, hexose; HexNAc, N-acetylhexosamine; QC, quality control; UGGT1, uridine 5′-diphosphate-glucose: glycoprotein glucosyltransferase 1; ER, endoplasmic reticulum; MS, mass spectrometry; LC, liquid chromatography; ConA, concanavalin A; EIC, extracted ion-chromatogram; CID, collision-induced dissociation.

* Corresponding authors. ERATO, Japan Science and Technology Agency (JST), Ito Glycotrilogy Project, 2-1 Hirosawa, Wako, Saitama 351-0198, Japan. Fax: +81 463 50 2432.
E-mail address: kanie@tokai-u.jp (O. Kanie).

http://dx.doi.org/10.1016/j.bbrc.2015.04.105
0006-291X/

attachment site [12]. In the course of our study, we recognized that the expression level of the protein affected the glycan structures. Thus, we recognized the need to investigate the glycan structures produced by different expression levels of this protein.

Recombinant glycoproteins are often used in research in the fields of biochemistry and molecular biology. Mammalian cell lines, especially Chinese hamster ovary (CHO) cells, have been extensively utilized for the production of recombinant glycoproteins [13,14]. However, the glycoform of glycoproteins produced by a cell is dependent on culture conditions and cell lines [15]. Hence, it is conceivable that glycoforms of recombinant and endogenous glycoproteins are distinguishable, resulting in considerable changes in biological activity. Thus, it is important to clarify whether the glycan structure of recombinant proteins is altered in comparison with endogenous proteins. Moreover, the relationship between the expression level of recombinant glycoproteins and their glycan structures is not clear.

Mass spectrometry (MS) is the most widely used analytical technique for glycosylation investigations [16–18]. In most cases, the glycan structures of glycoproteins are analysed as glycopeptides after digestion using protease(s). However, the detection of glycopeptides is often very difficult because the ionization efficiency of glycopeptides is lower than that of existing non-glycosylated peptides. To overcome this problem, various enrichment methods for glycopeptides have been developed, including lectin affinity and hydrophilic interaction chromatographies [19–21].

Herein, we report a relationship between *N*-linked glycan structures and the expression level of human recombinant UGGT1. In this analysis, tryptic digests of the UGGT1s were subjected to nano-liquid chromatography-tandem mass spectrometry (nano-LC–tandem MS). The results revealed that structural changes in *N*-linked glycans depend on glycoprotein expression levels, suggesting the importance of “quality control” of glycan structures in expressed glycoproteins.

2. Materials and methods

2.1. Expression of recombinant UGGT1 in human embryonic kidney (HEK) 293T cells

For various expression levels of human UGGT1 in HEK293T cells, we used pFN21K, pFN22K, pFN23K, and pFN24K HaloTag CMV Flexi Vectors (Promega, Tokyo, Japan), which are constructed to alter levels of expression level by modification of the CMV enhancer/promoter region. pFN21K allows the highest expression level, while pFN24K results in the lowest expression level. Signal peptide and 3 × FLAG-tag sequences of the pFLAG-CMV-9 expression vector (Sigma–Aldrich Japan, Tokyo, Japan) were inserted at the *N*-terminal side of the HaloTag protein for purification of recombinant proteins. cDNA encoding amino acids 38–1555 of human UGGT1 was inserted downstream of the HaloTag protein sequence, between the SgfI and PmeI restriction sites. The construct positioned the ER-retention signal of UGGT1 at the *C*-terminus of the recombinant protein. The plasmids were transfected into 293T cells using Lipofectamine 2000 (Life Technologies Japan, Tokyo, Japan) according to the manufacturer's instructions. After 48 h, the cells were harvested and the recombinant proteins were purified using Anti-FLAG M2-agarose (Sigma–Aldrich Japan, Tokyo, Japan) as described previously [22].

2.2. Cell imaging to define the expression level and localization of UGGT1

HEK293T cells were grown in Dulbecco's modified Eagle medium (D-MEM) containing 10% (v/v) fetal bovine serum (Life Technologies Japan, Tokyo, Japan), penicillin, and streptomycin. The cells were maintained at 37 °C in 5% CO_2.

Immunofluorescence analysis was performed on paraformaldehyde-fixed HEK293T cells using mouse monoclonal antibody against protein disulfide isomerase (PDI, Abcam, Tokyo, Japan) and Alexa Fluor® 680-conjugated goat anti-mouse IgG antibody (Life Technologies Japan, Tokyo, Japan) for dual staining to confirm UGGT1 localization.

HEK293T cells were cultured in 35-mm glass bottom culture dishes (Matsunami Glass Ind., Ltd., Osaka, Japan) coated with collagen (Cellmatrix Type IV; Nitta Gelatin Inc., Osaka, Japan). These cells were grown to approximately 30–40% confluence as a monolayer. The cells were transfected with the indicated plasmids using Lipofectamine 2000 (Life Technologies Japan, Tokyo, Japan), according to the manufacturer's protocol.

After 6 h exposure to the plasmid/Lipofectamine complex, the cells were incubated for 36 h with fresh growth medium. After rinsing three times with pre-warmed phosphate buffered saline (PBS), the cells were incubated with HaloTag® Oregon Green® ligand (final concentration, 1.0 μM) in D-MEM for 40 min at 37 °C in 5% CO_2, washed three times with PBS, and further incubated in fresh medium for 40 min. The cells were gently washed with PBS, fixed in 4% (w/v) paraformaldehyde for 15 min at room temperature, and then permeabilised for 10 min with PBS containing 1% (w/v) saponin and 0.1% (w/v) normal goat serum (NGS). Cells were then blocked in blocking buffer [10% (w/v) NGS in PBS] for 30 min at room temperature and incubated with anti-PDI antibody (diluted 1/100) for 1 h at room temperature. Next, the cells were incubated with the respective goat Alexa Fluor® 680-conjugated goat secondary IgG (1:200 in PBS containing 0.5% BSA) for 1 h at room temperature. Between steps, extensive washes (3 × 20 min) with PBS were performed to remove unbound reagents. The cells were then mounted onto glass slides using ProLong Gold Antifade Reagent (Invitrogen) with Hoechst 33342 (diluted 1/1000; Molecular Probes®) for staining of the nucleus. Immunofluorescence was detected using an Olympus FluoView FV1000-D laser scanning confocal microscope with a UPLSAPO oil-immersion objective lens (60×, Neofluar objective = 1.35; Olympus). In addition to a taking a differential interference contrast (DIC) image, the sample was sequentially excited using a 405 nm, 473 nm, and 635 nm laser and the fluorescence signal in the blue (422 nm), green (526 nm), or red (668 nm) channel, respectively, was recorded. A co-localization analysis of the expression of the recombinant protein with the ER marker PDI was performed using Olympus FluoView software (version 3.1a).

2.3. Preparation of recombinant UGGT1 from HEK293T cells

To obtain recombinant UGGT1s from HEK293T cells, we used the method described in a previous report [12]. Rough ER fractions were extracted from HEK293T cells using an Endoplasmic Reticulum Enrichment Kit (Imagenex Technologies Co., Washington, USA) according to manufacturer's instruction. Extracted rough ERs were dissolved in the binding buffer (20 mM Tris–HCl (pH 7.4), 500 mM NaCl, 1 mM $MnCl_2$, 1 mM $CaCl_2$, and 5% (v/v) Triton X-100). To remove contaminant proteins, these solutions were subjected to concanavalin A (ConA)-Sepharose (ConA) (GE Healthcare Japan, Tokyo, Japan) affinity chromatography according to the following process. After diluting 10 times with the binding buffer, these solutions (1.5 mL) were applied to the column. After washing with 30 mL of the washing buffer (20 mM Tris–HCl (pH 7.4), 500 mM NaCl, 1 mM $MnCl_2$, and 1 mM $CaCl_2$), UGGTs were eluted with 30 mL of the elution buffer (20 mM Tris–HCl (pH 7.4), 500 mM NaCl, and 300 mM methyl D-glucopyranoside). Eluents were concentrated to 300 μL using Amicon 30K (Millipore).

2.4. SDS-PAGE and in-gel digestion

UGGT1s obtained by affinity chromatography were subjected to reduction and carbamidomethylation, and were separated on NuPAGE 4–12% Bis-Tris Gel (Life Technologies Japan, Tokyo, Japan). The protein was visualized by Quick CBB staining (Wako Pure Chemicals Ind. Ltd., Osaka, Japan). The molecular weight of UGGT1s was estimated based on Novex® Sharp Unstained Protein Standards (Life Technologies Japan, Tokyo, Japan). An in-gel digestion was performed using the following procedure. The excised gel bands were destained with 30% acetonitrile, shrunk with 100% acetonitrile, and dried in a SpeedVac Concentrator. The dried gels were incubated with Sequencing Grade Modified Trypsin (Promega, Tokyo, Japan) at 50 °C for 3 h in 40 mM ammonium bicarbonate (pH 8.0). Peptides were extracted from the gels with 60% acetonitrile containing 0.1% trifluoroacetic acid under sonication for 15 min and concentrated with a vacuum concentrator.

2.5. NanoLC and MS conditions

For the separation of tryptic digestion samples of UGGT1_21–24, the Nano Frontier nLC digital nanoflow HPLC system (Hitachi High-Technologies, Tokyo, Japan) was utilized. A tapered capillary column was used as a sprayer tip for ionization and was filled with C18 silica particles (particle size: 3 μm; 75 μm I.D. × 150 mm L.; Nikkyo Technos Co., Ltd., Tokyo, Japan). Mobile phase A was water containing 0.1% formic acid, whereas mobile phase B was acetonitrile containing 0.1% formic acid (LC-MS grade) (Merck Japan, Tokyo, Japan). The proportion of mobile phase B was programmed to linearly increase from 10% to 50% for 60 min and increase to 100% at 60.1 min. Samples dissolved in water-acetonitrile (9:1) containing 0.1% formic acid and 0.05% trifluoroacetic acid were used for injection. Other analytical conditions were as follows: flow rate, 200 nL/min; injection volume, 3 μL; separation and room temperature, approximately 25 °C.

Tryptic digestion samples of UGGT1_21–24 were analysed using a quadrupole ion trap mass spectrometer (QIT-MS) coupled with a nanoelectrospray interface (amaZon ETD; Bruker Daltonics). The parameters for analysis were (1) dry temperature, 120 °C; (2) dry gas (N_2), 4.0 L/min; (3) scan range, m/z 500–2250 (MS) and m/z 200–2500 (MS/MS); (4) compound stability, 100%; (5) target mass, m/z 1650; (6) ion charge control (ICC), on, target 200,000; (7) maximum accumulation time, 200 ms; (8) average, 5 spectra; (9) polarity, positive; (10) isolation width, m/z 4.0, and (11) end-cap radio frequency amplitude, 1.2 V.

2.6. Database searching

MS/MS data analysis was performed using the Data Analysis program (Bruker Daltonics). Automated matching to an interpreted database was performed via the internet using MASCOT (http://www.matricsience.com/) [23].

3. Results and discussion

3.1. Localization of recombinant UGGT1s in the cultured HEK293T cells

In this investigation, UGGT1s were expressed as recombinant proteins fused with a purification tag and a HaloTag for later visualization. Because of the presence of these extra amino acids, however, the localization of UGGT1s had to be confirmed. This confirmation process also provided information on any localization changes with different levels of protein expression. Thus, the cultured cells were exposed to HaloTag® Oregon Green® ligand and then fixed with paraformaldehyde containing saponin, and the ER was immunostained using anti-PDI antibody and Alexa Fluor® 680-conjugated goat secondary IgG. The nuclei were also stained with Hoechst 33342. As is clearly shown in Fig. 1A, the expressed UGGT1s co-localized with the ER marker, indicating that the expressed proteins were localized at the ER. The expression levels also corresponded with the base length in the promoter region (Fig. 1A and B). In the cases of pFN23K- and pFN24K-tagged UGGT1s, however, some cells with high UGGT1 expression levels were sporadically observed. Based on these observations, the expressed UGGT1s were considered to be eligible for the glycoform analysis, and the sporadic observations of high expression were expected to have a negligible impact on the results because of the thousands of cells that were analysed.

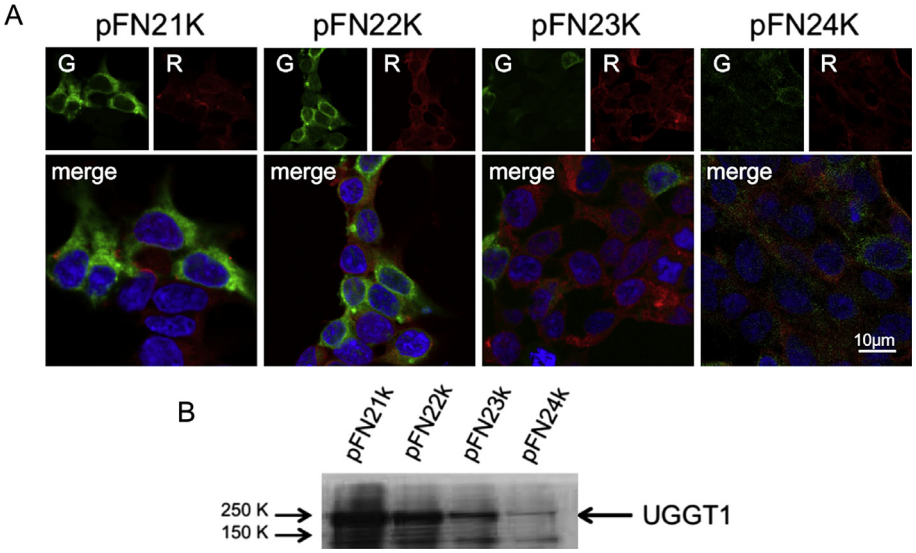

Fig. 1. A: Localization analysis of expressed HaloTag-fused uridine 5′-diphosphate-glucose: glycoprotein glucosyltransferase 1 (UGGT1). UGGT1 (green), protein disulfide isomerase (PDI; red), nucleus (blue). B: Confirmation of the expression level of HaloTag-fused UGGT1 protein based on SDS-PAGE.

3.2. Purification and identification of recombinant UGGT1s

For the successful structural analysis of glycan modifications on a particular glycoprotein, it is essential to purify the glycoprotein from tissues and cells prior to the mass spectrometric investigation. Contamination of other proteins in an analyte makes structural analysis of a glycoprotein extremely difficult. Thus, the most used method relies on the expression of a recombinant protein carrying a peptide tag(s), such as $(His)_n$- or FLAG-tags [24]. We expressed recombinant UGGT1s with an FLAG-Tag. The expression levels of UGGT1s were controlled with vectors that were constructed with different lengths in the CMV enhancer/promoter (expression level: pFN21K > pFN22K > pFN23K > pFN24k) [25]. Identification of the glycan structure of each UGGT1 expressed by using a series of vectors consisting of the above CMV enhancer/promoter sequences was accomplished by a procedure described in our previous report. This method consists of proteolytic digestion and MS/MS analysis. In this study, we prepared four recombinant glycoproteins, namely UGGT1_21 (pFN21K), UGGT1_22 (pFN22K), UGGT1_ 23 (pFN23k), and UGGT1_24 (pFN24k) in cultured HEK293T cells, for glycan structural analysis after tryptic digestion. The endogenous glycan structures of UGGT1 expressed in HEK293T cells were used as the control.

In order to purify each UGGT1 protein, we performed anti-FLAG M2-agarose affinity chromatography. Proteins were then separated by SDS-PAGE and visualized in the gel with Coomassie Brilliant Blue (CBB). Bands appearing at an approximate molecular weight of 220 kDa were considered to be UGGT1s (ca. 160 kDa) fused with HaloTag (ca. 60 kDa), according to the theoretical molecular weights (Fig. 1B). These bands were excised from the gel, and the mixtures of peptides and glycopeptides that were obtained by in-gel digestion using trypsin were subjected to nanoLC-MS and MS/MS analysis. The MS/MS ion search in MASCOT for the peptide mixtures obtained in this manner identified these bands to be UGGT1_human (Fig. 1). A flow chart detailing the process of protein identification using MASCOT is shown in Fig. 2.

3.3. Structural analysis of N-glycans from UGGT1_21–24

It is important to clarify whether oligosaccharyltransferase, which catalyses the transfer of Glc3Man9GlcNAc2 glycan to nascent polypeptides in the ER, can efficiently act on nascent recombinant UGGT1 polypeptide. In a previous report, a structural analysis of glycans of UGGT1_293T was performed using a quadrupole ion-trap mass spectrometer (QIT-MS) [12]. Therefore, the same platform was used for the analysis in this study.

Since UGGT1 is an ER-resident glycoprotein, recombinant UGGT1s are thought to contain high-mannose type glycans. The backbone peptide sequences of glycopeptide fragments of recombinant UGGT1s produced by tryptic digestion were ^{265}GTEVNTTVIGENDPIDEVQGFLFGK^{289}, ^{529}IGFIFVVNDSEDVDGMQDAGVAVLR^{553}, and ^{1213}ADMVNEDLLSDGTSENESGFWDSFK^{1237}, whose molecular weights were calculated to be 2678, 2665, and 2792 Da, respectively. Peaks detected at around 81 min in the nanoLC-MS were speculated to contain several hexoses, including two HexNAcs and ^{265}GTEVNTTVIGENDPIDEVQGFLFGK^{289}, according to the calculated m/z value (Fig. 3A). As for the glycopeptides, triply charged ion species $[M+3H]^{3+}$ were observed. The difference in the mass number between these peaks was 54 ($z = 3$), which corresponded to one hexose, indicating that these peaks represented glycopeptides. In order to clarify the glycan structures at detected peaks, we performed an MS/MS analysis for these peaks. Fig. 3C shows the resulting MS/MS spectrum of m/z 1354. Y-ion signals (m/z 1030, 1084, 1138, 1192, 1246, and 1300) appeared as a result of the cleavage of carbohydrate units from the non-reducing end of the glycan structure. We observed a predominant Y1-ion, which was a product of glycosyl cleavage between two *N*-acetyl-D-glucosamine residues (m/z 1442). In addition, we observed m/z 528, 690, 852, 1014, and 1176 corresponding to $[HexNAc + Hex_{2-6} + H]^+$, respectively. These ion species are known to be very useful for providing glycan structures under MS/MS conditions when glycopeptides are being analysed. Therefore, a series of ions with m/z 1300, 1354, 1408, 1408, and 1462 are Hex_{5-8}-$HexNAc_2$-peptide, respectively. As a result of MS and MS/MS, UGGT1_21 with a peptide sequence of ^{265}GTEVNTTVIGENDPIDEVQGFLFGK^{289} was found to only have *N*-linked glycans at N269. Other peptides, including the consensus sequence Asn-X-Ser/Thr, X≠ Pro, were not detected in this analysis. This result was the same as that found for UGGT1_293T in our previous report. In addition, non-glycosylated ^{265}GTEVNTTVIGENDPIDEVQGFLFGK^{289} peptide was not detected (data not shown). Therefore, it was concluded that recombinant UGGT1 was fully *N*-glycosylated at N269, similar to endogenous UGGT1, even when the recombinant protein was over-expressed (see Fig. 4).

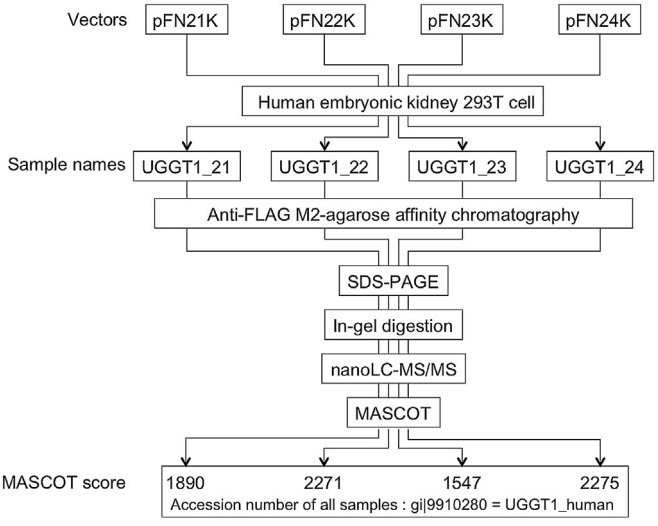

Fig. 2. Flow chart for the identification of UGGT1s.

3.4. N-glycan structures of recombinant UGGT1s in different level of expression

In order to understand the relationship between the glycan structure attached to recombinant UGGT1 and the expression level of the protein, we compared the glycan structures of UGGT1_21, _22, _23, and _24 at each expression level. We also explored whether glycans attached to recombinant UGGT1 exhibited the same structures as those attached to endogenous UGGT1. A semi-quantitative analysis was performed using the peak area of the extracted ion chromatograph (EIC). Representative chromatograms are shown in Fig. 3B. It has been reported that the ionization properties of individual glycopeptides are dominated by the peptide portion [26,27]. In the current investigation, a peak observed in the total ion chromatogram (TIC) consisted of glycopeptides sharing identical peptide sequences but possessing various glycans, indicating that the relative amounts of the individual glycoforms could be estimated. In our previous report, UGGT1_293T had predominantly Man_5-and Man_6-type glycans [12]. This indicated that the glycan of UGGT1_293T was cleaved by ER-resident mannosidase. In the cases of UGGT1s_21–24, detected glycans carried Hex_{5-8} that corresponded to Man_{5-8}-type glycans (Fig. 3A). In addition, with higher protein expression (UGGT_21), the protein

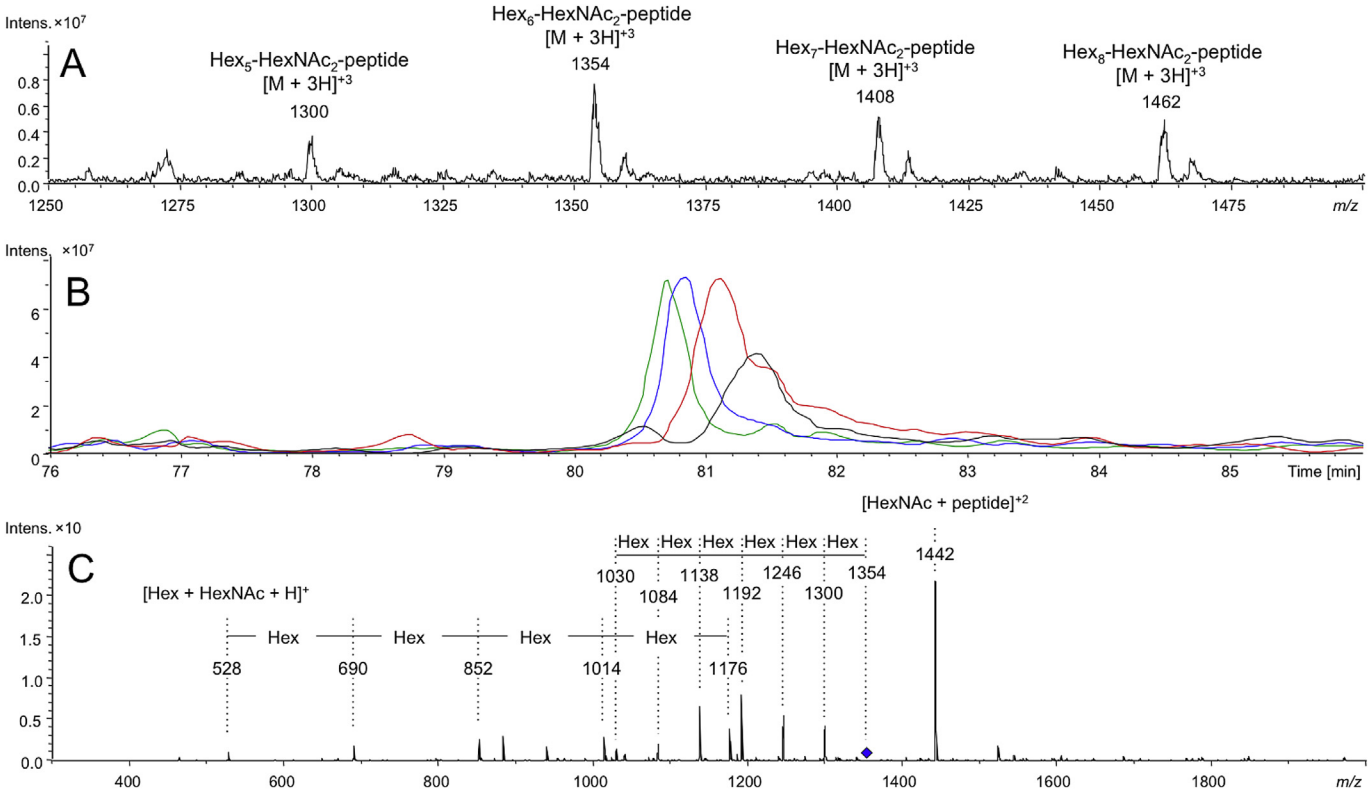

Fig. 3. Determination of glycan structure in UGGT1. A: MS spectrum for a peak in nanoLC at around 81 min showing glycosylated peptide fragment ions with *m/z* 1300 ($Hex_5HexNAc_2$-peptide), *m/z* 1354 ($Hex_6HexNAc_2$-peptide), *m/z* 1408 ($Hex_7HexNAc_2$-peptide), and *m/z* 1462 ($Hex_8HexNAc_2$-peptide). B: EIC analysis of UGGT1_21. Black: *m/z* 1300 ($Hex_5HexNAc_2$-peptide); red: *m/z* 1354 ($Hex_6HexNAc_2$-peptide); blue: *m/z* 1408 ($Hex_7HexNAc_2$-peptide); green: *m/z* 1462 ($Hex_8HexNAc_2$-peptide). C: A typical MS/MS spectrum of a glycopeptide ($Hex_5HexNAc_2$-peptide) from UGGT1_21 showing a ladder of signals corresponding to the structure.

had a longer *N*-glycan attachment than endogenous UGGT1-293T. These results suggested that a considerable portion of UGGT1_21 remained, probably reflecting the reaction rates of peptide synthesis and ER-mannosidase. However, when the expression amount was low (UGGT1_24), the *N*-glycans attached to recombinant UGGT1 were similar to the endogenous glycan structure. These results indicated that the *N*-linked glycan structure of UGGT1 is intimately dependent on the expression level of the polypeptide chain.

3.5. Concluding remarks

A relationship between the protein expression levels under forced expression and the glycoform of an ER-resident glycoprotein UGGT1 was clearly shown. It may be premature to discuss a generality of the phenomenon, however, it is easily understood that the type of changes can occur when larger amount of polypeptides are synthesised because of the imbalance in reaction rates for the peptide synthesis and glycan triming. Furthermore, since the

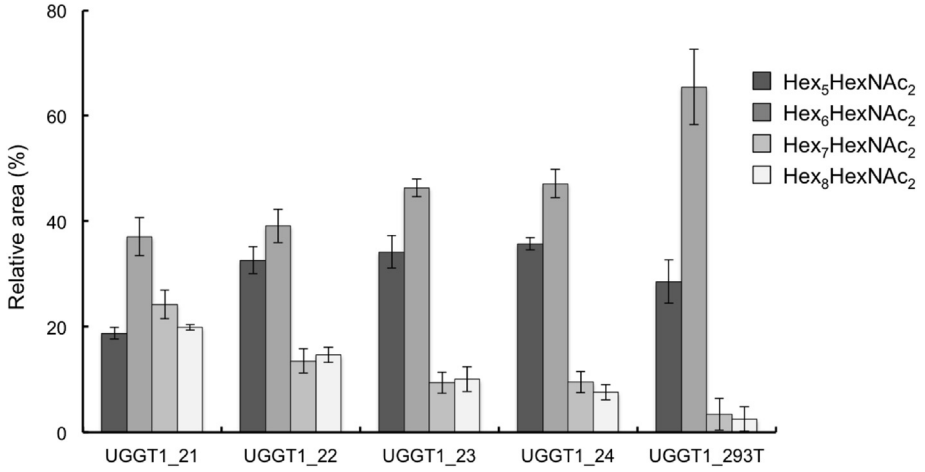

Fig. 4. Relative quantity of glycan chains found in each UGGT1. The relative quantities were obtained from extracted ion chromatograms shown in Fig. 3B.

trimming reaction at ER is the foundation of glycan synthesis at Golgi apparatus, the type of insufficient trimming at ER may affect the overall glycoform of glycoproteins produced. The increase of high-mannose type glycan structures in cancer cells is considered to correlate with our findings [28,29]. Thus, it is considered that glycoproteins without ER-retension signal may also undergo insufficient trimming of mannose residues, and are secreted or are transferred to plasma membrane.

It is known that changes in glycan structure can alter the physiological function of a protein, even if the primary structure of the protein remains unchanged [30]. Hence, it is important to confirm glycan structures for an accurate analysis of glycoprotein function. In this study, we expressed an ER-resident glycoprotein, UGGT1, at different levels in HEK293T cells, in order to allow an accurate analysis of its function. Our results indicated that UGGT1 glycan structures were related to the protein expression level, suggesting a way to control for a glycan profile similar to the endogenous UGGT1. It is expected that structural and functional analyses of *N*-linked glycans on ER-resident glycoproteins having the same glycoform as that on their endogenous counterparts can be performed following this method.

Conflict of interest

We declare no conflict of interest.

Transparency document

Transparency document related to this article can be found online at http://dx.doi.org/10.1016/j.bbrc.2015.04.105.

References

[1] R. Apweiler, H. Hermjakob, N. Sharon, On the frequency of protein glycosylation, as deduced from analysis of the SWISS-PROT database, Biochim. Biophys. Acta 1473 (1999) 4–8.
[2] R.A. Dwek, Glycobiology: toward understanding the function of sugars, Chem. Rev. 96 (1996) 683–720.
[3] J.C. Egrie, J.K. Browne, Development and characterization of novel erythropoiesis stimulating protein (NESP), Nephrol. Dial. Transpl. 16 (2001) 3–13.
[4] A. Beck, T. Wurch, C. Bailly, N. Corvaia, Strategies and challenges for the next generation of therapeutic antibodies, Nat. Rev. Immunol. 10 (2010) 345–352.
[5] S. Elliott, T. Lorenzini, S. Asher, K. Aoki, D. Brankow, Enhancement of therapeutic protein in vivo activities through glycoengineering, Nat. Biotechnol. 21 (2003) 414–421.
[6] C.E. Warren, Glycosylation, Curr. Opti. Biotechnol. 4 (1993) 596–602.
[7] A. Helenius, M. Aebi, Roles of N-linked glycans in the endoplasmic reticulum, Annu. Rev. Biochem. 73 (2004) 1019–1049.
[8] S. Dejgaard, J. Nicolay, M. Taheri, D.Y. Thomas, J.J.M. Bergeron, The ER glycoprotein quality control system, Curr. Issues Mol. Biol. 6 (2004) 29–42.
[9] A.J. Parodi, Protein glucosylation and its role in protein folding, Annu. Rev. Biochem. 69 (2000) 69–93.
[10] A. Zapun, C.A. Jakob, D.Y. Thomas, J.J.M. Bergeron, Protein folding in a specialized compartment: the endoplasmic reticulum, Structure 7 (1999) R173–R182.
[11] C. Hammond, I. Braakman, A. Helenius, Role of N-linked oligosaccharide recognition, glucose trimming, and calnexin in glycoprotein folding and quality control, Proc. Natl. Acad. Sci. U. S. A. 91 (1994) 913–917.
[12] S. Daikoku, A. Seko, Y. Ito, O. Kanie, Glycan structure and site of glycosylation in the ER-resident glycoprotein, uridine 5'diphosphate-glucose: glycoprotein glucosyltransferases 1 from rat, porcine, bovine, and human, Biochem. Biophys. Res. Commun. 451 (2014) 356–360.
[13] L. Chu, D.K. Robinson, Industrial choices for protein production by large-scale cell culture, Biochem. Eng. J. 12 (2001) 180–187.
[14] T. Lai, Y. Yang, S.K. Ng, Advances in mammalian cell line development technologies for recombinant protein production, Pharmaceuticals 6 (2013) 579–603.
[15] P. Hossler, S.F. Khattak, Z.J. Li, Optimal and consistent protein glycosylation in mammalian cell culture, Glycobiology 19 (2009) 936–949.
[16] M. Wuhrer, A.M. Deelder, C.H. Hokke, Protein glycosylation analysis by liquid chromatography–mass spectrometry, J. Chromatogr. B 825 (2005) 124–133.
[17] H. Wang, C.-H. Wong, A. Chin, A. Taguchi, A. Taylor, Integrated mass spectrometry–based analysis of plasma glycoproteins and their glycan modifications, Nat. Protoc. 6 (2011) 253–269.
[18] Y. Kanie, M. Yamamoto-Hino, Y. Karino, H. Yokozawa, S. Nishihara, Insight into the regulation of glycan synthesis in Drosophila chaoptin based on mass spectrometry, PLoS One 4 (2009) e5434.
[19] H. Kaji, H. Saito, Y. Yamauchi, T. Shinkawa, M. Taoka, Lectin affinity capture, isotope-coded tagging and mass spectrometry to identify N-linked glycoproteins, Nat. Biotech. 21 (2003) 667–672.
[20] Y. Takegawa, K. Deguchi, T. Keira, H. Ito, H. Nakagawa, Separation of isomeric 2-aminopyridine derivatized N-glycans and N-glycopeptides of human serum immunoglobulin G by using a zwitterionic type of hydrophilic-interaction chromatography, J. Chromatogr. A 1113 (2006) 177–181.
[21] L.R. Ruhaak, C. Huhn, W.J. Waterreus, A.R. de Boer, Christian Neusüss, et al., Hydrophilic interaction chromatography-based high-throughput sample preparation method for N-glycan analysis from total human plasma glycoproteins, Anal. Chem. 80 (2008) 6119–6126.
[22] Y. Takeda, A. Seko, M. Hachisu, S. Daikoku, M. Izumi, Both isoforms of human UDP-glucose:glycoprotein glucosyltransferase are enzymatically active, Glycobiology 24 (2014) 344–350.
[23] D.N. Perkins, D.J. Pappin, D.M. Creasy, J.S. Cottrell, Probability-based protein identification by searching sequence databases using mass spectrometry data, Electrophoresis 20 (1999) 3551–3567.
[24] J. Nilsson, S. Ståhl, J. Lundeberg, M. Uhlén, P.Å. Nygren, Affinity fusion strategies for detection, purification, and immobilization of recombinant proteins, Protein Expr. Purif. 11 (1997) 1–16.
[25] M. Slater, D. Hartzell, J. Hartnett, S. Wheeler, P. Stecha, et al., Achieve the protein expression level you need with the mammalian HaloTag® 7 Flexi® Vectors, Promega Notes 100 (2008) 16–18.
[26] Y. Wada, P. Azadi, C.E. Costello, A. Dell, R.A. Dwek, et al., Composition of the methods for profiling glycoprotein glycan-HUPO human disease glycomics/proteomics initiative multi-institutional study, Glycobiology 17 (2007) 411–422.
[27] D. Kolarich, F. Altmann, E. Sunderasan, Structural analysis of the glycoprotein allergen Hev b 4 from natural rubber latex by mass spectrometry, Biochem. Biophys. Acta 1760 (2006) 715–720.
[28] T.G. Johns, I. Mellman, G.A. Cartwright, G. Ritter, L.J. Old, A.W. Burgess, A.M. Scott, The antitumor monoclonal antibody 806 recognizes a high-mannose form of the EGF receptor that reaches the cell surface when cells over-express the receptor, FEBS J. 19 (2005) 780–782.
[29] M.L.A. de Leoz, L.J.T. Young, H.J. An, S.R. Kronewitter, J. Kim, S. Miyamoto, A.D. Borowsky, H.K. Chew, C.B. Lebrilla, High-mannose glycans are elevated during breast cancer progression, Mol. Cell. Proteomics 10 (2011). M110.002717.
[30] C.H. Chung, B. Mirakhur, E. Chan, Q.T. Le, J. Berlin, Cetuximab-induced anaphylaxis and IgE specific for galactose-α-1,3-galactose, N. Engl. J. Med. 358 (2008) 1109–1117.